Unilateral Power Gain of an Optically Biased GaAs MESFET

By Srikanta Bose, Adarsh Gupta and R.S. Gupta
University of Delhi

The use of optical radiation to control the various functions and operations of gallium arsenide MESFETs has been the focus of intense research for several years. It has been shown that microwave characteristics of MESFETs can be controlled by incident optical radiation with photon energy greater than or equal to the bandgap energy in the same way as varying the gate bias in conventional electrically controlled MESFETs [1-6]. Optically biased FETs have many potential applications, such as high-speed optical detectors and converters for interaction of optical and microwave signals. The optimum noise figure of optically controlled GaAs MESFETs is lower than conventional MESFETs [5]. Therefore, high-speed, low cost, monolithically integrated optically gated GaAs MESFETs are in high demand for high-frequency application in optical communication systems.

This article discusses an analytical model that predicts the microwave characteristics of an optically biased GaAs MESFET. Admittance and scattering parameters are extracted and the unilateral power gain and maximum stable gain are evaluated; both show a significant improvement under illumination.

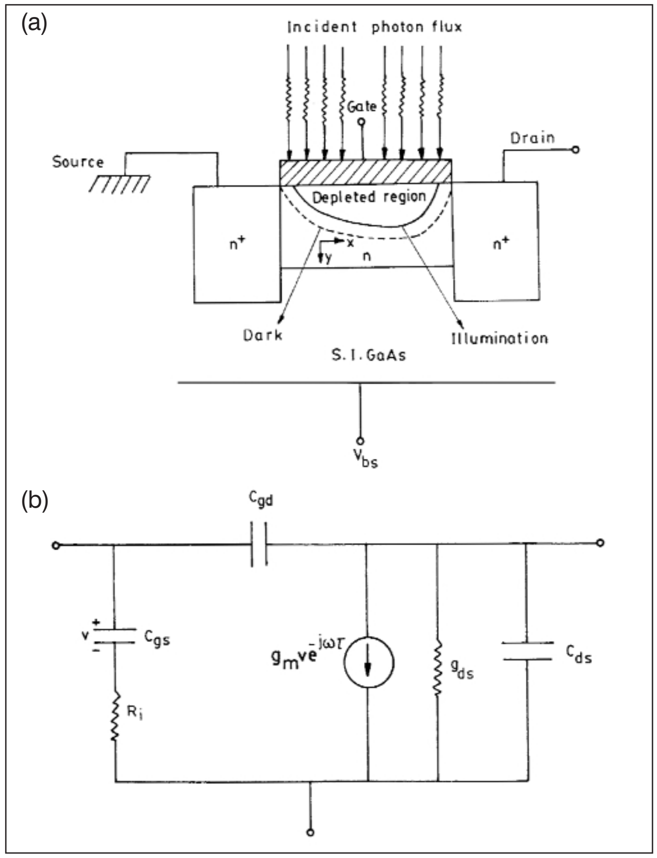

▲ **Figure 1. (a) Schematic structure of optically biased GaAs MESFET with active channel profile under dark (P_{opt} = 0) and illuminated conditions. (b) Equivalent circuit model for GaAs MESFET.**

Theoretical consideration

The schematic structure of an optically biased GaAs MESFET with active channel profile under dark and illuminated conditions is shown in Figure 1(a). Light radiation is allowed to fall on the gate metal along the vertical y-direction. The equivalent circuit model used to extract admittance and scattering parameters is shown in Figure 1(b).

The intrinsic *Y*-parameters for the optically biased GaAs MESFET in terms of equivalent circuit elements are given as:

$$Y_{11} = \frac{R_i\left(qZL\left(F_1'' + F_2''\right) + \frac{\pi}{2}\varepsilon Z\right)^2 \omega^2}{1 + R_i^2\left(qZL\left(F_1'' + F_2''\right) + \frac{\pi}{2}\varepsilon Z\right)^2 \omega^2} + j\omega\left(\frac{qZL\left(F_1'' + F_2''\right) + \frac{\pi}{2}\varepsilon Z}{1 + R_i^2\left(qZL\left(F_1'' + F_2''\right) + \frac{\pi}{2}\varepsilon Z\right)^2 \omega^2} + qZL\left(F_1''' + F_2'''\right) + \frac{\pi}{2}\varepsilon Z\right) \quad (1)$$

$$Y_{12} = -j\omega\left(qZL\left(F_1''' + F_2'''\right) + \frac{\pi}{2}\varepsilon Z\right) \quad (2)$$

$$Y_{21} = \left(\frac{\left(\frac{q\mu_n ZQ}{2L}\left(-\frac{2}{3}F_1' - \frac{2}{3}F_2'\right) + \left(\frac{q\mu_n Z\phi\tau_n}{L}\right)\left(\frac{qN_{eq}}{\varepsilon\alpha}\right)F_{3'} + \left(\frac{q\mu_p Z}{L}\right)\left(\frac{R\tau_p}{a}\right)\left(\frac{2\varepsilon}{qN_{eq.}}\right)^{\frac{1}{2}}F_4'\right)\exp(-j\omega\tau)}{1 + jR_i\left(qZL\left(F_1'' + F_2''\right) + \frac{\pi}{2}\varepsilon Z\right)\omega}\right) - j\omega\left(qZL\left(F_1''' + F_2'''\right) + \frac{\pi}{2}\varepsilon Z\right) \quad (3)$$

$$Y_{22} = g_{ds} + j\omega\left(C_{ds} + qZL\left(F_1''' + F_2'''\right) + \frac{\pi}{2}\varepsilon Z\right) \quad (4)$$

where

$$F_1' = V_1\frac{3}{2}\left(2a_p\left(\frac{2Na}{Q}\right)\left(\frac{2\varepsilon}{qN_a}\right)^{\frac{1}{2}}\frac{1}{2}\left(V_{bi} - V_{bs} + V_p\right)^{-\frac{1}{2}} - \frac{1}{V_1}\right) \times \left(\left(a_p^2 + \frac{V_{ds} - V_p}{V_1}\right)^{\frac{1}{2}} - \left(a_p^2 - \frac{V_p}{V_1}\right)^{\frac{1}{2}}\right) \quad (5)$$

$$F_2' = V_2\frac{3}{2}\left(-2\left(\alpha' + 1 - a_p\right)\left(\frac{2N_a}{Q}\right)\left(\frac{2\varepsilon}{qN_a}\right)^{\frac{1}{2}}\frac{1}{2}\left(V_{bi} - V_{bs} + V_p\right)^{-\frac{1}{2}} - \frac{1}{V_2}\right) \times \left(\left(\alpha' + 1 - a_p\right)^2 + \frac{V_{ds} - V_p}{V_2}\right)^{\frac{1}{2}} - \left(\left(\alpha' + 1 - a_p\right)^2 + \frac{V_p}{V_2}\right)^{\frac{1}{2}} \quad (6)$$

$$F_3' = \left(\frac{2\varepsilon}{qN_{eq.}}\right) \times \left(\frac{\alpha}{2}\right)\left(\exp\left(-\alpha\left(\frac{2\varepsilon}{qN_{eq.}}\right)^{\frac{1}{2}}\left(V_{bi}' + V_{ds} - V_{gs} - V_{op}\right)^{\frac{1}{2}}\right)\right) + \left(\exp\left(-\alpha\left(\frac{2\varepsilon}{qN_{eq.}}\right)^{\frac{1}{2}}\left(V_{bi}' - V_{gs} - V_{op}\right)^{\frac{1}{2}}\right)\right) + \left(\frac{q\mu_n Z\phi\tau_n}{L}\right)\left(\frac{qN_{eq.}}{\varepsilon\alpha}\right) \times \left(2\left(\frac{2\varepsilon}{qN_{eq.}}\right)^{\frac{1}{2}}\frac{1}{2\left(V_{bi}' - V_{gs} - V_{op}\right)^{\frac{1}{2}}}\right)\left(\exp\left(-\alpha\left(\frac{2\varepsilon}{qN_{eq.}}\right)^{\frac{1}{2}}\left(V_{bi}' - V_{gs} - V_{op}\right)^{\frac{1}{2}}\right)\right) \quad (7)$$

$$F_4' = \left(V_{bi}' + V_{ds} - V_{gs} - V_{op}\right)^{\frac{1}{2}} - \left(V_{bi}' - V_{gs} - V_{op}\right)^{\frac{1}{2}} \quad (8)$$

$$F_1'' = \frac{Q}{2}\left(-\left(\frac{1}{2}\right)\left(a_p{}^2 + \frac{V_{ds}-V_p}{V_1}\right)^{-\frac{1}{2}}\left(2a_p\left(\frac{2N_a}{Q}\right)\left(\frac{2\varepsilon}{qN_a}\right)^{\frac{1}{2}}\frac{1}{2}\left(V_{bi}-V_{bs}+V_p\right)^{-\frac{1}{2}} - \frac{1}{V_1}\right)\right) -$$
$$\frac{Q}{2}\left(-2\left(\alpha' + 1 - a_p\right)\left(\frac{2N_a}{Q}\right)\left(\frac{2\varepsilon}{qN_a}\right)^{\frac{1}{2}}\frac{1}{2}\left(V_{bi}-V_{bs}+V_p\right)^{-\frac{1}{2}} - \frac{1}{V_2}\right) \quad (9)$$

$$F_2'' = \frac{1}{2}\left(\frac{2\varepsilon}{qN_{eq.}}\right)^{\frac{1}{2}}\left(V_{bi}' + V_{ds} - V_{gs} - V_{op}\right)^{-\frac{1}{2}}\left(\phi\tau_n\alpha\left(\exp\left(-\alpha\left(\frac{2\varepsilon}{qN_{eq.}}\right)^{\frac{1}{2}}\left(V_{bi}' + V_{ds} - V_{gs} - V_{op}\right)^{\frac{1}{2}}\right)\right) - \frac{R\tau_p}{a}\right) \quad (10)$$

$$F_1''' = \frac{Q}{2}\left(-\left(\frac{1}{2}\right)\frac{1}{V_1}\left(a_p{}^2 + \frac{V_{ds}-V_p}{V_1}\right)^{-\frac{1}{2}} - \frac{1}{V_2}\right) \quad (11)$$

$$F_2''' = \frac{1}{2}\left(\frac{2\varepsilon}{qN_{eq.}}\right)^{\frac{1}{2}}\left(V_{bi}' + V_{ds} - V_{gs} - V_{op}\right)^{-\frac{1}{2}} \times$$
$$\left(\phi\tau_n\alpha\left(\exp\left(-\alpha\left(\frac{2\varepsilon}{qN_{eq.}}\right)^{\frac{1}{2}}\left(V_{bi}' + V_{ds} - V_{gs} - V_{op}\right)^{\frac{1}{2}}\right)\right) - \frac{R\tau_p}{a}\right) \quad (12)$$

where

- q is the electron charge
- ε is the permittivity of the semiconductor
- Q is the implanted ion dose
- a is the active layer thickness
- N_a is the substrate doping concentration
- $N_{eq.}$ is the equivalent doping concentration
- ϕ is the incident photon flux
- $\tau_{n,p}$ is the life time of electron (hole)
- R is the surface recombination rate
- α is the absorption coefficient per unit length
- V_{gs} is the gate to source voltage
- V_{ds} is the drain-source voltage
- V_{bs} is the substrate to source voltage
- V_{bi}' is the built in potential at Schottky gate contact
- V_{op} is the photovoltage developed at the Schottky junction due to illumination
- $\mu_{n,p}$ is the electron (hole) mobility
- Z is the device width
- L is the gate length
- R_i is the charging resistance
- V_{bi} is the built in voltage

and

$$V_1 = \frac{qQ^2}{8N_a\varepsilon}$$

$$V_2 = \frac{qQ\sigma}{\sqrt{2\pi}\varepsilon}$$

$$a_p = \frac{2N_a}{Q}\sqrt{\frac{2\varepsilon}{qN_a}\left(V_{bi}-V_{bs}+V_p\right)}$$

and

$$\alpha' = \frac{R_p}{2\sigma}\sqrt{\frac{\pi}{2}}$$

where R_p is the projected range parameter of the implanted Gaussian profile and σ is the straggle parameter of the implanted Gaussian profile, V_p is the pinchoff voltage, g_{ds} is the device output conductance, C_{ds} is the drain-source capacitance, $\omega = 2\pi f$, Y_{11} and Y_{22} are the input and output admittance parameters, Y_{12} is the reverse transfer admittance parameter and Y_{21} is the forward transfer admittance parameter.

The corresponding S-parameters for optically biased GaAs MESFET are

$$S_{11} = \frac{A_1^- B_1^+ + C_1}{A_1^+ B_1^- - C_1} \quad (13)$$

$$S_{12} = \frac{D_1}{A_1^+ B_1^- - C_1} \quad (14)$$

$$S_{21} = \frac{E_1}{A_1^+ B_1^- - C_1} \quad (15)$$

$$S_{22} = \frac{A_1^+ B_1^- + C_1}{A_1^+ B_1^- - C_1} \quad (16)$$

where

$$A^{\pm}{}_1 = 1 \pm \frac{R_i\left(qZL\left(F_1'' + F_2''\right) + \frac{\pi}{2}\varepsilon Z\right)^2 \omega^2}{1 + R_i^2\left(qZL\left(F_1'' + F_2''\right) + \frac{\pi}{2}\varepsilon Z\right)^2 \omega^2} \pm j\omega\left(\frac{qZL\left(F_1'' + F_2''\right) + \frac{\pi}{2}\varepsilon Z}{1 + R_i^2\left(qZL\left(F_1'' + F_2''\right) + \frac{\pi}{2}\varepsilon Z\right)^2 \omega^2} + qZL\left(F_1''' + F_2'''\right) + \frac{\pi}{2}\varepsilon Z\right) \quad (17)$$

$$B^{\pm}{}_1 = 1 \pm g_{ds} \pm j\omega\left(C_{ds} + qZL\left(F_1''' + F_2'''\right) + \frac{\pi}{2}\varepsilon Z\right) \quad (18)$$

$$C_1 = -jw\left(qZL\left(F_1''' + F_2'''\right) + \frac{\pi}{2}\varepsilon Z\right) \times \left(\frac{\left(\frac{q\mu_n ZQ}{2L}\left(-\frac{2}{3}F_1' - \frac{2}{3}F_2'\right) + \left(\frac{q\mu_n Z\phi\tau_n}{L}\right)\left(\frac{qN_{eq.}}{\varepsilon\alpha}\right)F_3' + \left(\frac{q\mu_p Z}{L}\right)\left(\frac{R\tau_p}{a}\right)\left(\frac{2\varepsilon}{qN_{eq.}}\right)^{\frac{1}{2}} F_4'\right)\exp(-j\omega\tau)}{1 + jR_i\left(qZL\left(F_1'' + F_2''\right) + \frac{\pi}{2}\varepsilon Z\right)\omega}\right) - \omega^2\left(qZL\left(F_1''' + F_2'''\right) + \frac{\pi}{2}\varepsilon Z\right)^2 \quad (19)$$

$$D_1 = 2j\omega\left(qZL\left(F_1''' + F_2'''\right) + \frac{\pi}{2}\varepsilon Z\right) \quad (20)$$

$$E_1 = -2 \times \left(\frac{\left(\frac{(q\mu_n ZQ)}{2L}\left(-\frac{2}{3}F_1' - \frac{2}{3}F_2'\right) + \left(\frac{q\mu_n Z\phi\tau_n}{L}\right)\left(\frac{qN_{eq.}}{\varepsilon\alpha}\right)F_3' + \left(\frac{q\mu_p Z}{L}\right)\left(\frac{R\tau_p}{a}\right)\left(\frac{2\varepsilon}{qN_{eq.}}\right)^{\frac{1}{2}} F_4\right)\exp(-j\omega\tau)}{1 + jR_i\left(qZL\left(F_1'' + F_2''\right) + \frac{\pi}{2}\varepsilon Z\right)\omega}\right) + 2j\omega\left(qZL\left(F_1''' + F_2'''\right) + \frac{\pi}{2}\varepsilon Z\right) \quad (21)$$

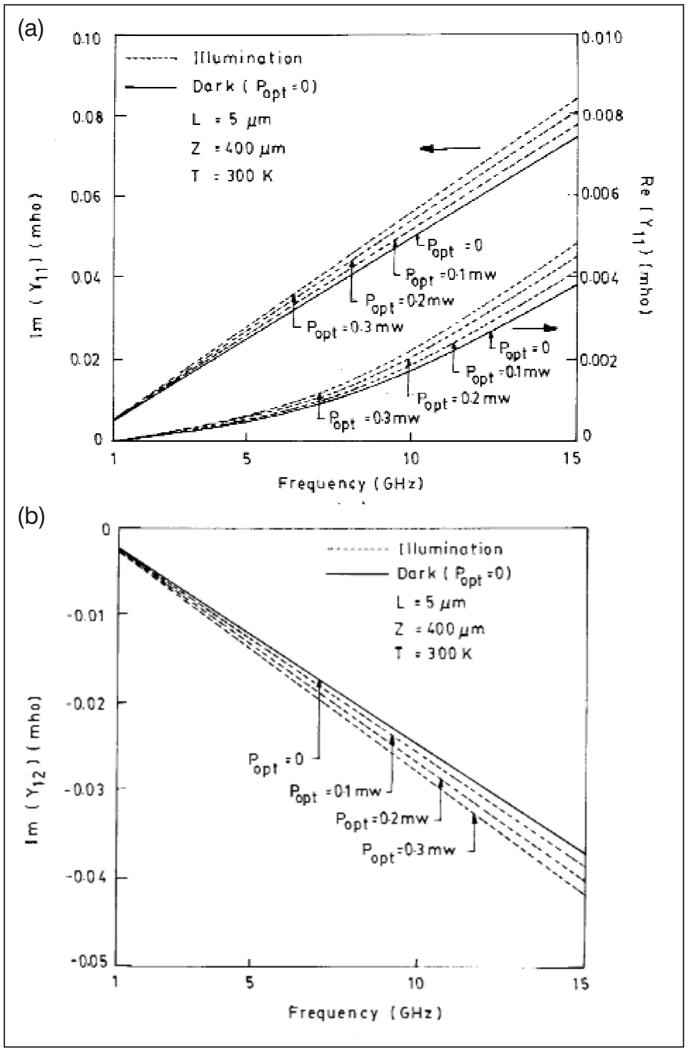

▲ **Figure 2. (a) Input admittance parameter variation with frequency under dark (P_{opt} = 0) and illuminated conditions [Q = 1.5 × 10^{16} /m^2, R_p = 8.61 × 10^{-8} m, σ = 3.83 × 10^{-8} m, λ = 0.827 x 10^{-6} m, a = 0.25 μm, R_i = 2.69 Ω, N_a = 10^{20}/m^3, k_n = 3.1 × 10^{-15} m^3/s, k_p = 3.1 × 10^{-17} m^3/s]. (b) Reverse transfer admittance parameter variation with frequency under dark (P_{opt} = 0) and illuminated conditions.**

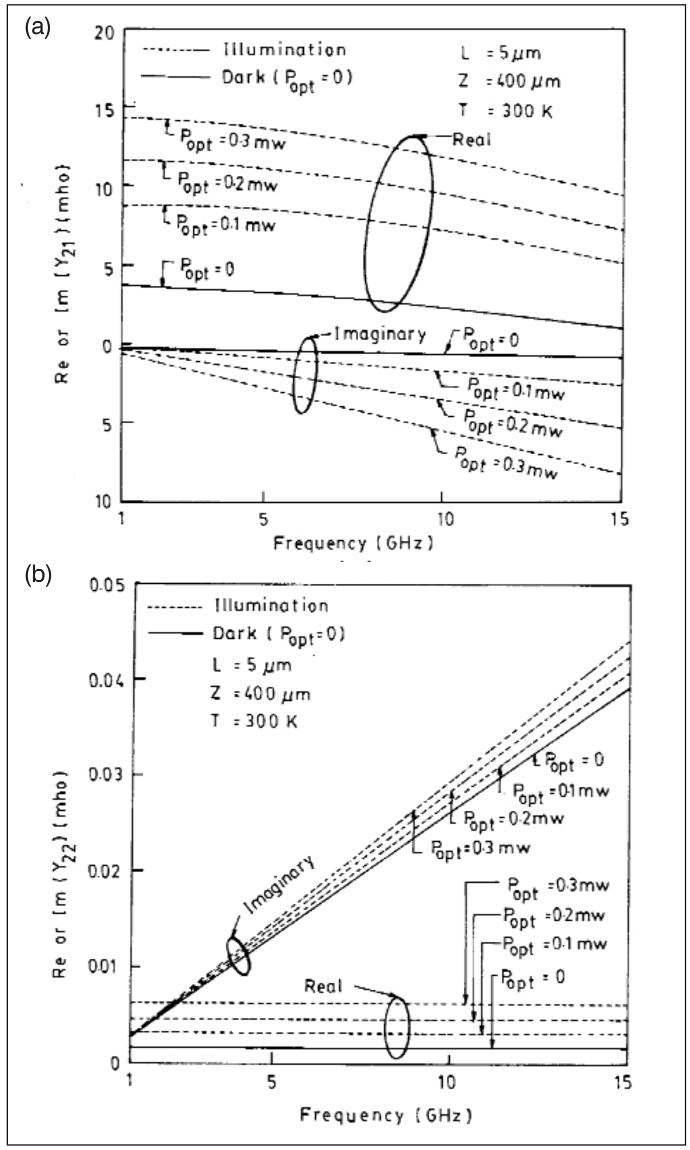

▲ **Figure 3. (a) Forward transfer admittance parameter variation with frequency under dark (P_{opt} = 0) and illuminated conditions. (b) Output admittance parameter variation with frequency under dark (P_{opt} = 0) and illuminated conditions.**

The unilateral power gain (UPG) and maximum stable gain (MSG) are calculated using the relation

$$U = \frac{|Y_{21} - Y_{12}|^2}{4\left[\mathrm{Re}(Y_{11})\mathrm{Re}(Y_{22}) + \mathrm{Re}(Y_{12})\mathrm{Re}(Y_{12})\right]} \quad (22)$$

$$MSG = \frac{|S_{21}|}{|S_{12}|} \quad (23)$$

Results and discussion

Figures 2 and 3 show the variation of admittance parameters with frequency under dark and illuminated conditions. Figure 2(a) shows that under the illuminated condition, Y_{11} improves when the device is exposed to light radiation and a photovoltage is developed across the Schottky junction. This voltage effectively reduces the barrier height, and the depletion layer width decreases. The channel width increases reducing the channel resistance and increasing the channel conductance. The same trend is observed in other Y-parameters. The parameter Y_{21}, which primarily determines the gain of the device, shows a significant enhancement when illuminated, as shown in Figure 3(a).

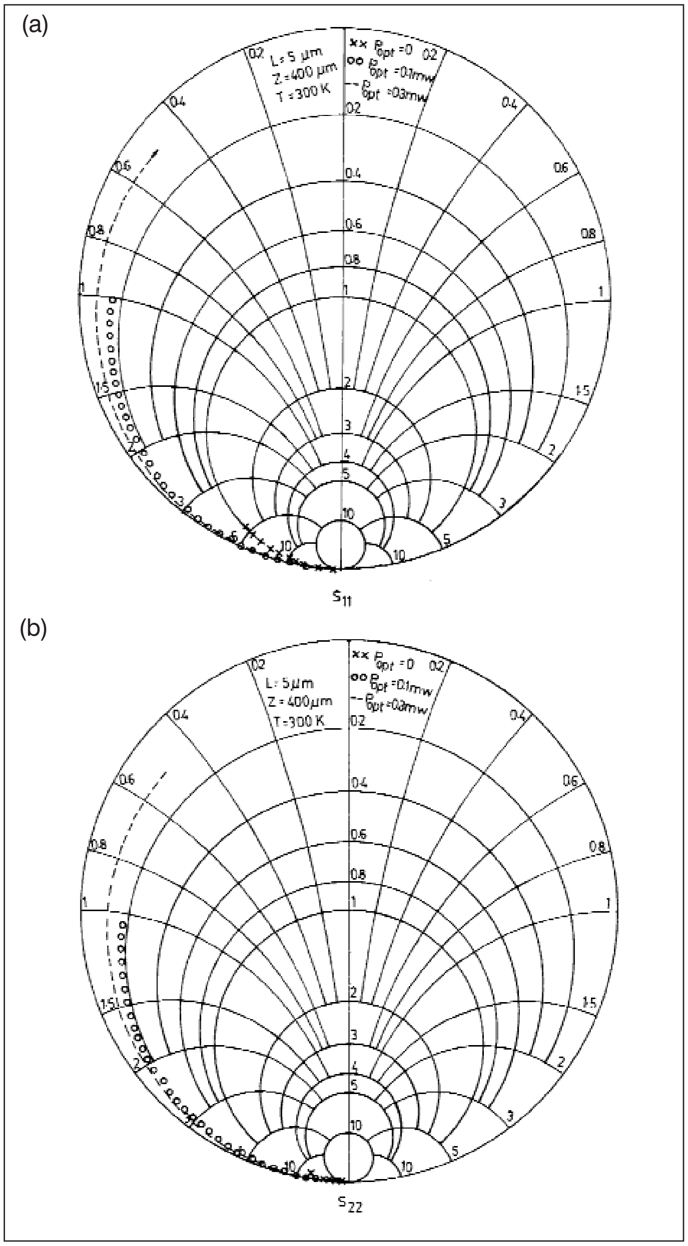

▲ **Figure 4. (a) Input reflection coefficient variation with frequency under dark (P_{opt} = 0) and illuminated conditions. (b) Output reflection coefficient variation with frequency under dark (P_{opt} = 0) and illuminated conditions.**

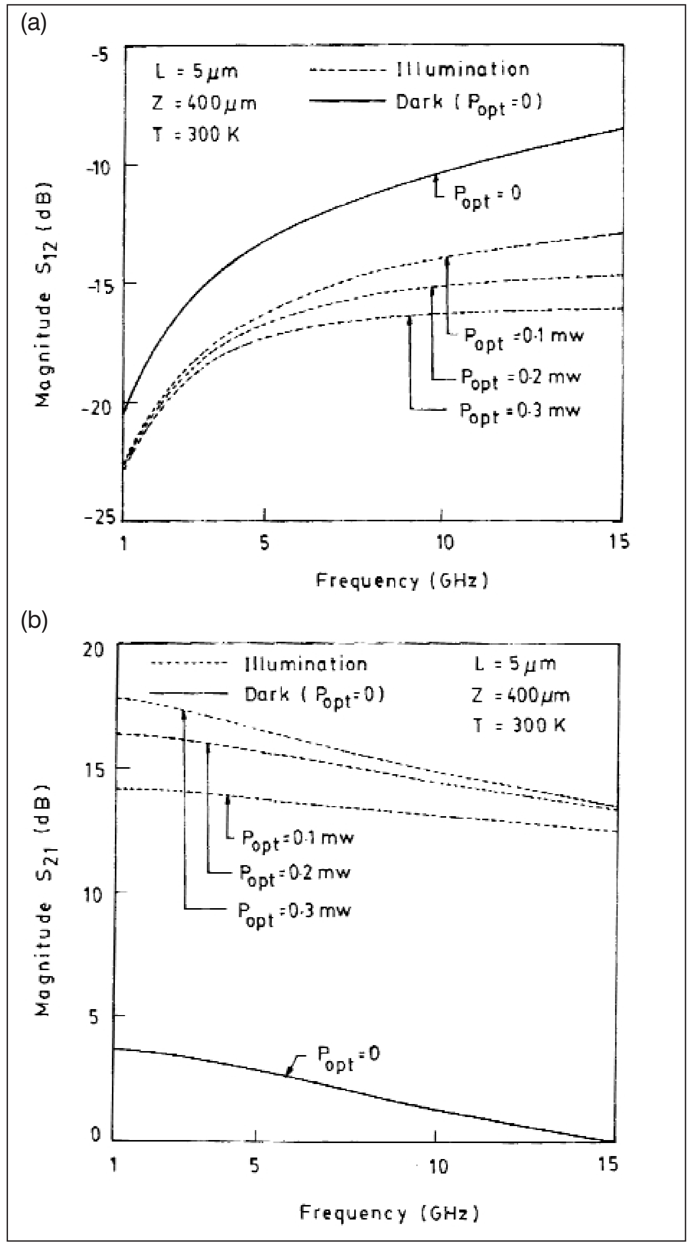

▲ **Figure 5. (a) Reverse transmission coefficient variation with frequency under dark (P_{opt} = 0) and illuminated conditions. (b) Forward transmission coefficient variation with frequency under dark (P_{opt} = 0) and illuminated conditions.**

Figures 4 and 5 show the variation of scattering parameters under dark and illuminated conditions. The reflection coefficients S_{11} and S_{22} are plotted on the Smith chart in Figure 4, which iillustrates the improvement in loss under illumination. Figure 5(a) shows that the reverse transmission coefficient S_{12}, is smaller under illumination compared to when under dark condition. The forward transmission coefficient S_{21} shows an almost 10 dB improvement under illumination (for example, for P_{opt} = 0.1 mW), as shown in Figure 5(b). The cause for this change is mainly the transconductance of the device, which increases under illumination [5].

Figure 6 shows the variation of unilateral power gain with frequency under dark and illuminated conditions. For a given frequency, the UPG of the device increases significantly under illumination compared to dark condition. The MSG shown in inset also behaves in a similar fashion.

Conclusion

An analytical model has been developed to predict microwave characteristics of optically biased GaAs MESFET. The admittance and scattering parameters are evaluated analytically. The plots show that there is a noteworthy change in admittance and scattering parameters of the device under illumination. A significant improvement in UPG and MSG for the device is observed under illumination. Optically biased GaAs MESFETs promise potential for optical communication systems.

Acknowledgement

The authors wish to acknowledge the following institutions for providing the necessary financial support for this research: the University Grants Commission, Government of India; and DRDO, Ministry of Defense, Government of India. ■

References

1. C. Baack, G. Elze and G. Wolf, "GaAs MESFET: A high-speed optical detector," *Electronics Letters*, Vol. 13, 1977: 193.

2. A. DeSalles and J. R. Forest, *Applied Physics Letters*, Vol. 38, 1981: 392-394.

3. A. DeSalles, "Optical control of GaAs MESFETs," *IEEE Transactions on Microwave Theory and Techniques*, Vol. MTT-31, 1983: 812-820.

4. D.K.W. Lam and R.I. MacDonald, "GaAs optoelectronic mixer operation at 4.5 GHz," *IEEE Transactions on Electronic Devices*, Vol. ED-31, 1984: 1766-1768.

5. S. Bose, M. Gupta and R.S. Gupta, "Cutoff frequency and optimum noise figure of GaAs optically controlled FET," *Microwave Opt Technology Letters*, Vol. 26, 2000: 279-282.

6. S. Bose, M. Gupta and R.S. Gupta, "Id ~ Vd characteristics of optically biased short channel GaAs MESFET," *Microelectronics Journal* (in press).

7. G.W. Taylor, H.M. Darley, R.C. Frye and P.K. Chatterjee, "A Device Model for an Ion-Implanted MESFET," *IEEE Transactions on Electronic Devices*, Vol. ED-26, 1979: 172-182.

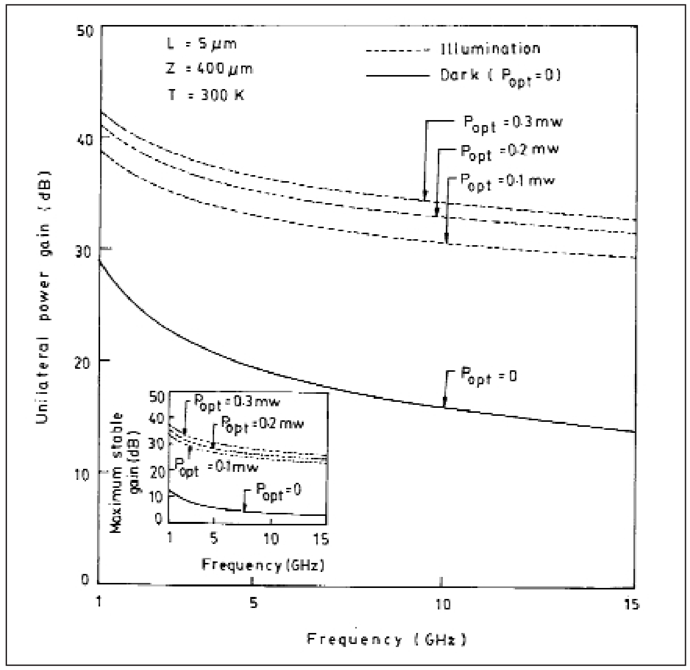

▲ **Figure 6. Unilateral power gain and maximum stable gain (inset) variation with frequency under dark (P_{opt} = 0) and illuminated conditions.**

Author Information

Srikanta Bose received a master of science degree in physics in 1995 from Ravenshaw College (Utkal University), with specialization in electronics. He joined the Department of Electronic Science at the University of Delhi, South Camus, in 1997 as a junior research fellow under the University Grant Fellowship Scheme, Government of India, to pursue a Ph.D. His research interest includes modeling and simulation of solid state microelectronic devices (MESFET/OPFET/HEMT/MOSFET) for high frequency applications. He has published 15 papers in various international journals and conferences. Currently, he is at the Institute of Electro-Optical Engineering, NCTU, Hsinchu, Taiwan, as a post-doctoral research scientist. He can be reached via E-mail: srbose@usa.net; Tel: +0091-11-4105580; or Fax: +0091-11-6886606.

Adarsh Gupta received a master of science degree in physics from the University of Delhi, New Delhi, India, in 2000. She has been a Ph.D. student at the Department of Electronic Science, University of Delhi, South Camus, since 2000 under the DRDO (Defense Research & Development Organization) Project, Government of India. Her area of research includes modeling and simulation of GaN MESFETs for microwave frequency applications. She has published two papers in international journals. She can be reached via E-mail: adarsh23@yahoo.com; Tel: +0091-11-4105580; or Fax: +0091-11-6886606.

R. S. Gupta is a senior faculty member in the Department of Electronic Science at the University of Delhi, South Camus. His research areas include modeling and simulation of solid state microelectronic devices (MESFET/OPFET/HEMT/MOSFET) for high frequency applications. He is a senior member of the IEEE. He has published more than 150 papers in in various international journals and conferences. He can be reached via E-mail: rsgu@bol.net.in; Tel: +0091-11-4105580; or Fax: +0091-11-6886606.